The Association Between the North Atlantic Oscillation and the Interannual Variability of the Tropospheric Transport Pathways in Western Europe

J.A.G. Orza **(Universidad Miguel Hernández)**
M. Cabello **(Universidad Miguel Hernández)**
V. Galiano **(Universidad Miguel Hernández)**
A.T. Vermeulen **(ECN)**
A.F. Stein **(Earth Resources Technology)**

June 2013
ECN-B--13-005

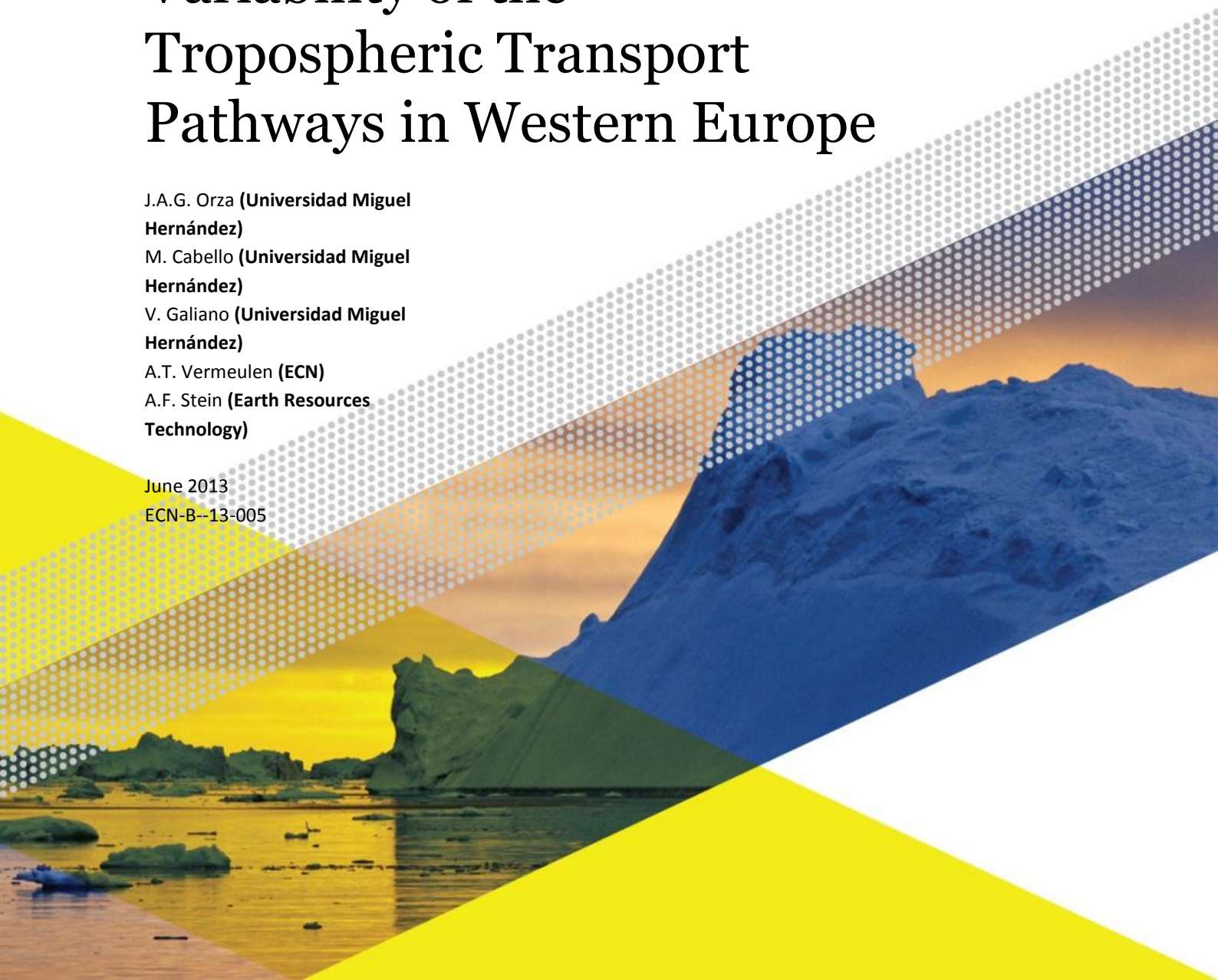

The Association Between the North Atlantic Oscillation and the Interannual Variability of the Tropospheric Transport Pathways in Western Europe

J. A. G. Orza,[1] M. Cabello,[1] V. Galiano,[1] A. T. Vermeulen,[2] and A. F. Stein[3,4]

The variations in tropospheric transport pathways over a 20 year period, 1990–2009, are studied at six locations in Europe. Three Atlantic (Lisbon, Mace Head, and Cabauw) and three Mediterranean sites (Málaga and Elche in the western part and Lecce in the central Mediterranean) are considered. The work is based on the identification of flow types at each location by robust cluster analysis of the trajectories, the assessment of temporal trends for each advection pattern, and subsequent quantification of the association, at the monthly scale, between the North Atlantic Oscillation (NAO) index (NAOi) and the frequency of occurrence of the identified flows. This exploratory study demonstrates the usefulness of the approach for specific locations in a context where synoptic circulation/weather-type classifications are usually used. A different number of advection pathways were identified at each location. Common features to all the sites were prevalence of westerly flows, strong seasonal variability, and association of the air flow types to known synoptic situations in both phases of the NAO. The degree of association varies strongly with latitude, location within the Mediterranean basin, and closeness to the action centers. Overall, flows reaching Mace Head and Cabauw present stronger association to the NAO, which is substantially reduced at lower latitudes and is not significant at Lisbon. Significant temporal trends are found for northerly flows at Mace Head and Málaga, associated to changes at the beginning of the study period that are also present in the NAOi time series. WSW flows at Mace Head exhibit a steady decreasing trend over the whole period.

1. INTRODUCTION

The North Atlantic Oscillation (NAO) is the dominant pattern of atmospheric circulation variability in the North Atlantic area, with influence in the climate of most Europe [e.g., *Hurrell*, 1995; *Hurrell and van Loon*, 1997], mainly during the winter season when the NAO is stronger. In the positive phase of the NAO, the Azores high-pressure center is stronger than usual, and the Icelandic low-pressure center is deeper. In winter, the positive phase is associated with a northward shift in the Atlantic storm activity, which causes dryer conditions in southern Europe. The NAO is in its negative phase when the opposite anomalies are found.

Several indices have been proposed to describe the NAO phenomenon and its temporal evolution [see *Pozo-Vázquez et al.*, 2000; *Jones et al.*, 2003]. In general, NAO index (NAOi) values are derived either from the difference in surface-level pressure anomalies between two locations near the NAO centers of action or from the application of principal component analysis to gridded surface pressure or tropospheric geopotential height data.

[1]SCOLAb, Física Aplicada, Universidad Miguel Hernández, Elche, Spain.
[2]Environmental Assessment, ECN-Energy Research Centre of the Netherlands, Petten, Netherlands.
[3]Earth Resources Technology, Inc., Laurel, Maryland, USA.
[4]NOAA's Air Resources Laboratory, NOAA, Silver Spring, Maryland, USA.

Lagrangian Modeling of the Atmosphere
Geophysical Monograph Series 200

10.1029/2012GM001315

Table 1. Location of the Study Sites

Site	Latitude (°N)	Longitude (°E)
Mace Head (Ireland)	53.317	−9.900
Cabauw (The Netherlands)	51.971	4.927
Lecce (Italy)	40.346	18.095
Lisbon (Portugal)	38.720	−9.130
Elche (Spain)	38.270	−0.700
Malaga (Spain)	36.730	−4.480

Changes in the NAOi have been correlated with changes in the frequency of occurrence of daily synoptic circulation/weather types, like those derived by automated Lamb weather classifications [*Sheridan*, 2003; *Lorenzo et al.*, 2008]. Here the use of air flow types identified by clustering of back trajectories is proposed, which allows studying trends in transport patterns at specific locations as well as the degree of association between the occurrence of each flow type and the NAOi. The use of back trajectories would show explicitly the transport pathways followed by air masses reaching a given study site, and include the influence of variation in atmospheric fields during the days the air parcels travel.

The analysis of back trajectories has been used successfully in environmental studies of long-range transport of pollutants and trace gases. Air trajectories have been utilized frequently for the qualitative interpretation of individual flow situations in relation to the measurements of various atmospheric constituents, and statistical methods that allow identifying geographic source regions and transport patterns from a large set of trajectories have become standard tools [*Ashbaugh et al.*, 1985; *Moody and Galloway*, 1988; *Dorling et al.*, 1992; *Stohl*, 1996; *Stohl and James*, 2004].

With respect to user-defined grouping of trajectories, statistical cluster analysis [*Moody and Galloway*, 1988; *Dorling et al.*, 1992] is a more objective approach. Moreover, grouping by geographical sectors does not take into account either the curvature or the length of the trajectories, which contain relevant information: e.g., short trajectories may be related to stagnant weather conditions, while high dispersion rates are associated to long trajectories. Cluster analysis of back trajectories has been applied to identify synoptic-scale atmospheric transport patterns [e.g., *Jorba et al.*, 2004; *Santese et al.*, 2008; *Hondula et al.*, 2010; *Markou and Kassomenos*, 2010]. But only a few studies have actually made a climatological (several decades) study of air flow types by clustering of back trajectories [*Kahl et al.*, 1997; *Delcloo and De Backer*, 2008]. The latter reported also a trend analysis of the relative occurrence of each cluster and of ozone concentration segregated by the identified clusters.

In the work presented here, six locations in Europe were selected to study the interannual variations in tropospheric transport pathways: three Atlantic locations (Lisbon, Mace Head, and Cabauw) and three Mediterranean sites (Málaga and Elche in the western part; Lecce in the central Mediterranean). Lisbon and the Mediterranean sites are located at similar latitudes, while Mace Head and Cabauw have more northerly locations (Table 1; see also Figure 1). Lisbon has the particular feature of being located inside the southern pressure system of the NAO.

Identification of the main pathways of advection at each location was performed by robust cluster analysis of the trajectories for a 20 year period. The interannual variability of the identified air flow types was explored at the monthly scale by trend analysis and the subsequent quantification of the association between the NAOi and the frequency of occurrence of the identified flows.

Already, studies exist on the origin and history of trajectories at the selected sites. Cluster analysis has been performed to interpret ozone concentrations in Mace Head by *Cape et al.* [2000] and *Tripathi et al.* [2010], to relate variations in aerosol size distribution close to Elche [*Cabello et al.*, 2008], and to analyze the transport pathways associated to naturally occurring radionuclides of either stratospheric or soil origin at Málaga [*Dueñas et al.*, 2011]. For Lecce [*Santese et al.*, 2008], trajectories were classified according to geographical sectors defined after a sensitivity study that used aerosol optical depth measures. Trajectories reaching Lisbon were also grouped according to geographical sectors by *Almeida et al.* [2005]. The influence of the different air flow patterns on the ambient radon concentrations at Cabauw has been studied for 2 months showing distinct transport conditions in the work of *Arnold et al.*

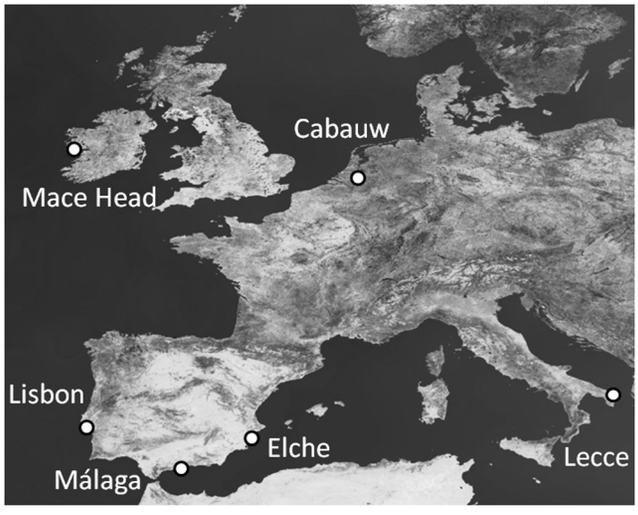

Figure 1. Location of the study sites. Top left and bottom right latitude and longitude of the map are 60°N, 13°W and 35°N, 20°E, respectively.

[2010] by a statistical analysis of large number of particles tracked backward with a Lagrangian particle dispersion (LPD) model. *Henne et al.* [2010] studied the Cabauw back trajectory footprint to analyze the spatial representativeness together with that of 33 other sites, and *Vermeulen et al.* [2011] presented the footprint for sensitivity to greenhouse gas emissions based on trajectory calculations. The work of *Tripathi et al.* [2010] identified the main air flow types reaching Mace Head from a back trajectory cluster analysis for a 20 year period, though trends in ozone concentration was done for trajectories combined into four main directions (compass sectors). The rest of those works considered much shorter study period.

The same meteorological database is used in this work to compute the trajectories for all the locations, and the same uniform clustering methodology is applied to all stations. In particular, the number of clusters at each site is obtained by applying the same criteria that eventually lead to a different number of clusters based solely on pathway similarity. As long as the factors that influence the air flow patterns and their complexity may vary from one site to another, an equal number of clusters for the studied locations is not to be expected.

Single-particle trajectory models do not fully account for turbulence and convective transport; therefore, they present limitations with respect to LPD models [see *Stohl*, 1998; *Stohl and Seibert*, 1998]. However, the statistical analysis of very large data sets of single-particle trajectories should reduce the uncertainties in the identification of the main transport pathways [*Brankov et al.*, 1998]; thus, the use of single trajectories was considered. Twenty years of particle dispersion calculations for a number of heights at several study sites, followed by cluster analysis, would be nearly unfeasible due to the needed computational resources, though that might result in a more robust characterization of the transport regimes.

2. METHODS AND DATA

2.1. Computation and Clustering of Back Trajectories

The Hybrid Single-Particle Lagrangian Integrated Trajectory (HYSPLIT) model version 4.8, from NOAA/ARL [*Draxler and Hess*, 1998], was used to compute daily 96 h backward trajectories starting at 12 UTC at three heights (500, 1500, and 3000 m above sea level) for the period 1990–2009. Meteorological fields from the European Centre for Medium-Range Weather Forecasts (ECMWF) reanalysis (ERA)-Interim data set [*Dee et al.*, 2011, http://data-portal.ecmwf.int/data/d/interim_daily/] were extracted and transformed to a 1.5° × 1.5° horizontal resolution, collapsed to 25 vertical levels and then used as input for the HYSPLIT model runs. The spatial resolution was chosen to keep moderate-sized data files. In particular, the vertical resolution was not reduced in the troposphere, as the lowest 20 vertical levels are the original lowest ERA-Interim (model) ones, which cover the whole troposphere. The three heights at each study location were restricted to the lower troposphere since our interest is mainly related to air quality.

The vertical movement of the air parcels was calculated using the vertical velocity field of the meteorological data. The resulting set for each of the six stations consisted of 7300 trajectories at each arrival height.

Trajectories were classified into homogeneous groups by a cluster procedure based on the k-means algorithm, with hourly longitude and latitude as input variables [*Moody and Galloway*, 1988]. The *k*-means algorithm groups a given data set into a certain number, k, of clusters, which must be fixed a priori, assigning each case to the best fitting cluster. A cluster is represented by its centroid, defined as the average over the trajectories belonging to that cluster. In a first step, k starting centroids are randomly chosen from the trajectory set. Once the trajectories have been allocated into the cluster to which centroid they are closest, the centroids are recalculated by averaging all the trajectories belonging to the same cluster, in an iterative process until no changes in cluster assignment are found.

The clustering result for a given k is known to present some dependence on the selected starting centroids, and it converges often to a local optimum. Therefore, 800 replicate clustering solutions were computed for that k, and the solution with the smallest total within-cluster sum of squared distances was retained as the best solution for that number of clusters. The use of a larger number of replicates does not improve further the solution.

Finally, the procedure followed to find out the optimal number of clusters was similar to the one of *Dorling et al.* [1992]. The number of clusters k was successively reduced by one, from 30 down to 3 clusters; for each k, the aforementioned 800 repetitions of the *k*-means clustering were made, and the best solution was the only one considered for that k. The total within-cluster mean squared distance between individual trajectories and their centroids was then examined as a function of the number of clusters. From this, the smallest number of clusters was retained for which the smallest percentage change in total RMSD is found when decreasing k by one. It should be noted that unlike *Dorling et al.* [1992], who reduced the number of clusters from k to $k - 1$ by merging the two closest centers, the clustering result for $k - 1$ clusters is here independent from that for k clusters.

The great-circle distance, i.e., the shortest distance measured along the surface of the sphere, was utilized as the similarity

measure in the clustering process, since the computation of Euclidean distances with geographical coordinates as planar would lead to errors that might not be acceptable at high latitudes.

2.2. NAO Index

There is no universally accepted NAOi to describe its temporal evolution. Monthly "station-based" indices of the NAO, produced by NCAR's Climate Analysis Section (https://climatedataguide.ucar.edu/sites/default/files/cas_data_files/asphilli/nao_station_monthly_0.txt) were utilized. They are computed from the difference of normalized sea level pressures between Ponta Delgada, Azores, and Stykkisholmur/Reykjavik, Iceland. Normalization at each station is done by division of each monthly pressure value by the long-term mean (1865–1984) standard deviation.

Charts of geopotential height at 700, 850, and 1000 hPa, averaged over the positive and the negative phases of the NAO for the whole study period, were produced from the ERA Interim database.

2.3. Temporal Trends and Association to the NAOi

The monthly time series considered in this work were examined for significant trends over the study period. A number of nonparametric statistical methods were conducted, mainly based on the Mann-Kendall (M-K) tau test to assess the significance of monotonic trends and the Theil-Sen (T-S) slope estimate for trend magnitude.

The significance of a trend is often overstated by serial correlation; but also, the presence of a trend alters the estimate of the serial correlation. Therefore, a first estimation of the correlation coefficients at different lags was done by computing the autocorrelation function (ACF) for each time series. The studied time series present, in general, some degree of serial correlation, in addition to seasonality; therefore, three methods of trend analysis were used with the aim of removing, or reducing, the influence of seasonality and lag-1 autocorrelation in the monthly data:

(1) The seasonal Kendall test [*Hirsch et al.*, 1982], which applies the M-K trend test separately for each month and then combines the results. (2) Aggregation of monthly data to annual means, and application of the M-K test to the resulting yearly time series. (3) The Yue-Pilon (Y-P) procedure [*Yue et al.*, 2002] applied to the previously deseasonalized monthly time series, to remove the influence of the month-to-month correlations in the significance of the trends. The Y-P procedure comprises several steps: the time series is linearly detrended using the T-S slope, and the serial autocorrelation of the residuals is removed. Then, the discarded linear trend is added back to the remaining time series, and the M-K test is applied.

Seasonal-trend decomposition of the time series was used to obtain the deseasonalized time series, which were subsequently analyzed by the Y-P procedure. The decomposition technique is based on a nonparametric regression technique (LOESS, locally weighted low-degree polynomial regression) recursively applied to the seasonal and trend components [*Cleveland et al.*, 1990]. Additionally, the (nonlinear, deseasonalized) trend component was used for the visual assessment of the long-term behavior of the time series.

The association between the extended-winter (from December to March, DJFM) means of the monthly frequencies of each air flow type and NAOi in the period 1990–2009 was examined via least-square regression analysis with statistical significance evaluated by a two-tailed t test. Since relationships need not be linear, the nonparametric Kendall rank test was also used to identify any statistically significant association without any a priori assumption of their form.

The trend analysis, as well as the association and significance tests, was conducted in R [*R Development Core Team*, 2010].

3. RESULTS

3.1. Transport Patterns and Variability

The cluster analysis identified the main pathways of advection to each of the six European sites. Between seven and four air flow types were found, depending on the location and the arrival height, with the smallest number for Elche, SE Spain. The representative trajectories (centroids) are shown in Figures 2 and 3.

Trajectory groups have been labeled according to their overall directions and length at each site. Therefore, air parcels of similar source region may have, in some cases, a different label. Specifically, polar maritime air masses advecting from the North Atlantic after passing over Labrador, Canada, are labeled as Wfast trajectories in Mace Head and Cabauw, while they are termed NWfast flows at lower latitudes.

Westerlies are predominant, as expected, given the general circulation in midlatitudes and are grouped into different transport patterns from northwesterlies (NW) to southwesterlies (SW) each with its characteristic length and curvature. Easterly (E)/northeasterly (NE) flows are grouped in one air flow type at each location. They are more frequent in the western Mediterranean, particularly at the lowest altitudes where they account for up to 44% of the trajectories. Slow flows are groupings of short trajectories, which are associated to weak synoptic forcing conditions. E/NE flows fall into

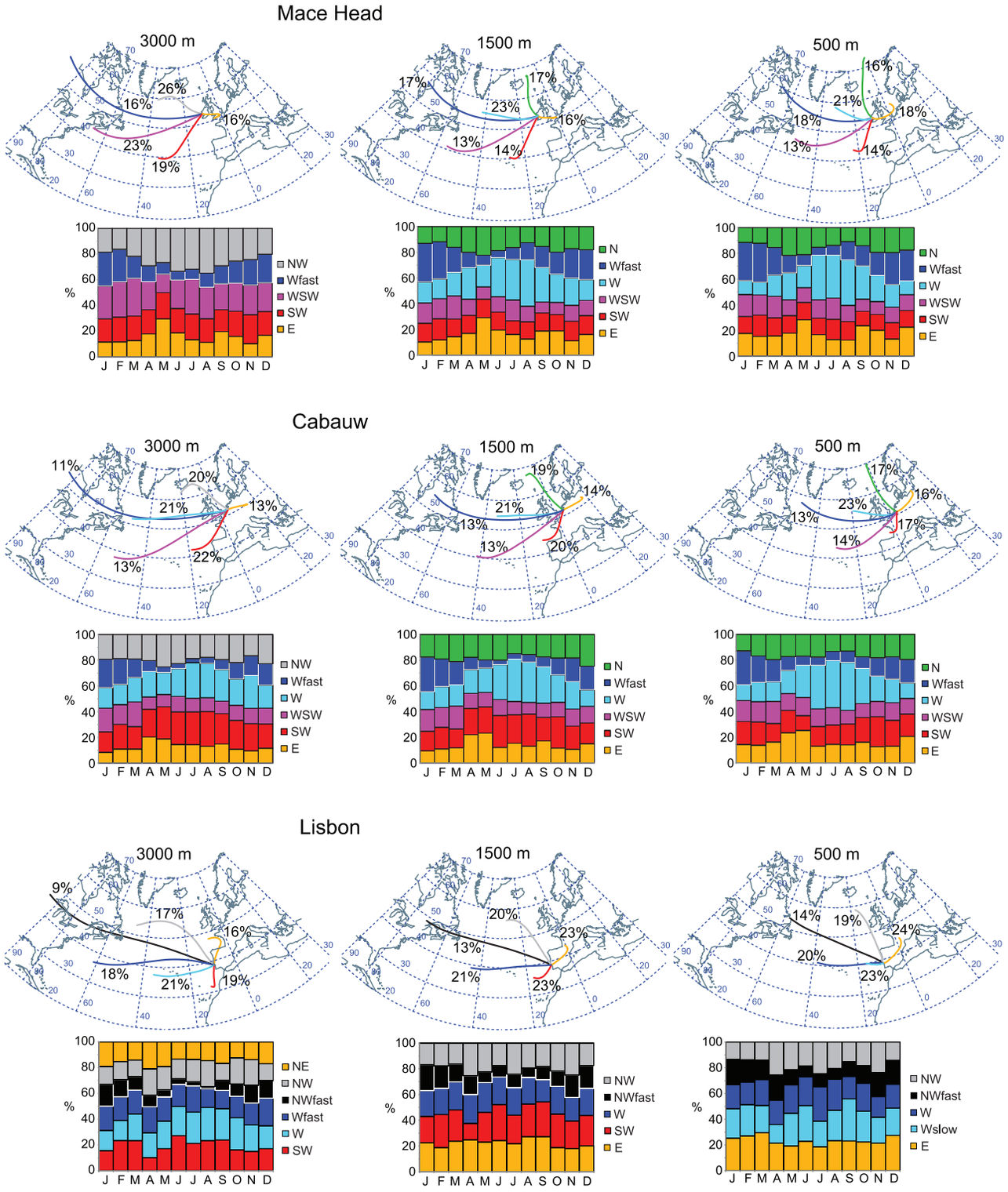

Figure 2. Representative trajectories (cluster centroids) of the air flow types arriving at (left) 3000 m, (middle) 1500 m, and (right) 500 m at the Atlantic sites, with their total percentage of occurrence. Below each trajectory plot, the monthly variation of the relative frequency of occurrence for each air flow type is shown.

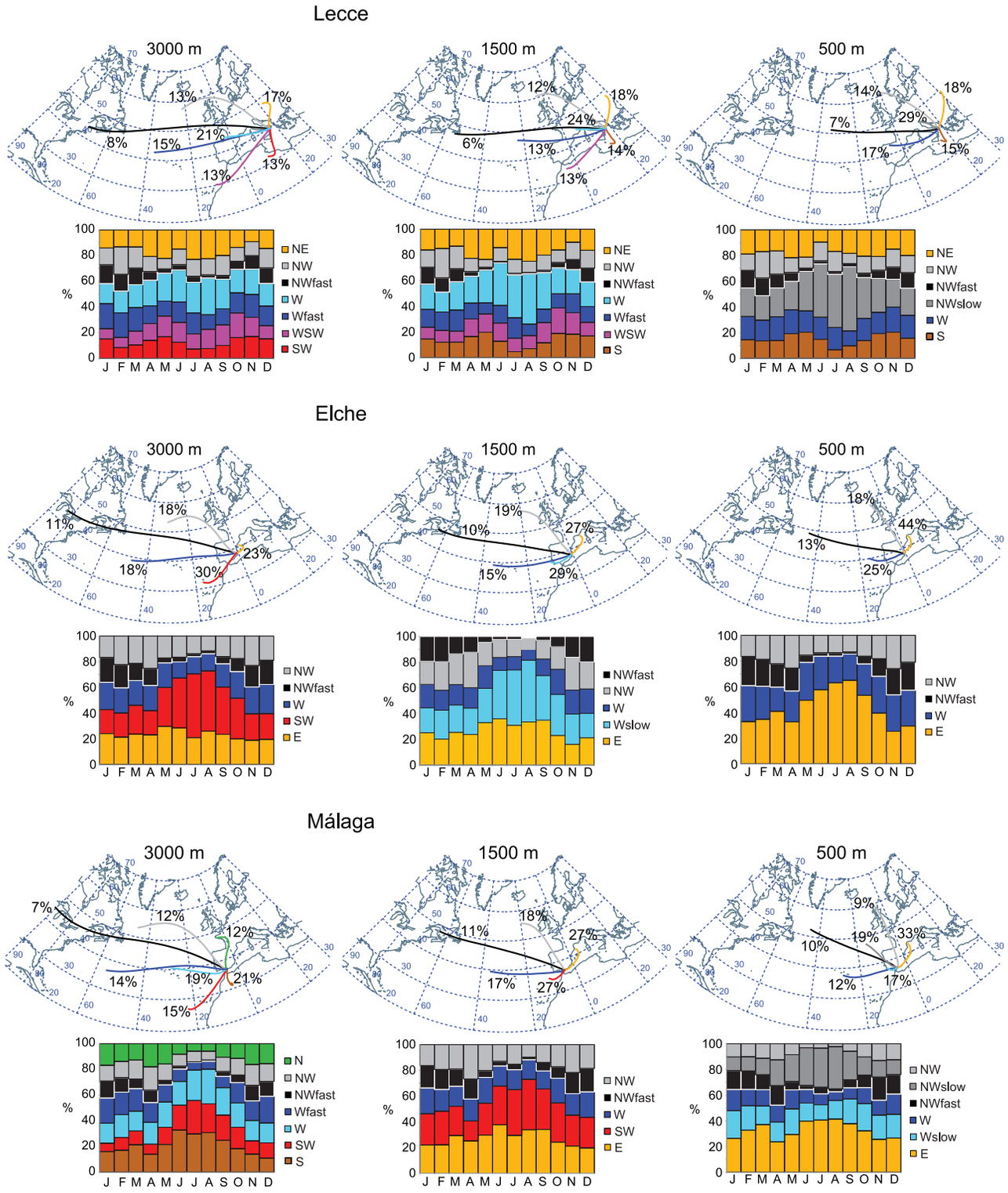

Figure 3. Representative trajectories (cluster centroids) of the air flow types arriving at (left) 3000 m, (middle) 1500 m, and (right) 500 m at the Mediterranean sites, with their total percentage of occurrence. Below each trajectory plot, the monthly variation of the relative frequency of occurrence for each air flow type is shown.

this class at all the sites, as do southerlies (S) at Lecce and at Málaga (at 3000 m), and SW at Elche, Málaga, Lisbon, and Cabauw (at 500m). At Lecce, there is an additional slow flow type with western and northern components, composed of trajectories passing over the Adriatic Sea or the Italian Peninsula from the Po basin.

The identified dominant transport patterns show clear seasonal dependence. The relative frequency of each air flow type for every month of the year is shown in Figures 2 and 3.

Wfast and W flows exhibit the greatest variance between months in Mace Head and Cabauw, followed by E/NE. Wfast flows are less frequent in the central months of the year, when slower W flows become more common. These two westerly advections are partially replaced by easterlies, which peak around March, December, and September–October. At the Mediterranean sites, polar maritime air flows present the same pattern being almost inexistent in summertime. Slow flows are more common in the central part of the year, with west component at Lecce (northwest at the lower height), and west and south components in the western Mediterranean at higher heights (while easterlies dominate at low altitudes). Southerlies are found in the transitional periods at Lecce and in summer at Málaga.

The seasonal nature of the arrival of fast polar maritime air at the different locations is also evidenced by the periodic behavior of the ACF of their monthly frequencies (not shown), with maxima and minima beyond bounds of significance (95% confidence) and a full cycle of 12 months. This behavior is shown at the three heights by the Wfast flows at Mace Head and Cabauw, as well as by NWfasts at Málaga, Elche, and Lecce. In Lisbon, it is only significant at 3000 m. That kind of periodicity is actually shared by the remaining advection patterns, which show strong seasonality due to marked differences in occurrence between the central part of the year and the rest, as can be appreciated in Figures 2 and 3: W flows reaching Mace Head at 1500 and 500 m, NWslows reaching Málaga at 500 m as well as S, SW, and Wfast flows arriving at 3000 m; Wslows arriving Elche at 1500 m and SW at 3000 m; NWslows reaching Lecce at 500 m, and Wslows at 1500 and 3000 m. It can be noted also that southerlies reaching Lecce at 500 m are the only case presenting a 6 month cycle in the ACF, according to their transitional nature. In the rest of the cases, however, serial correlations can be found at isolated lags and are just over the significance bounds. In a few cases, such correlation appears at lag-1 or lag-12, but no consistence between lags and air flow types or heights was found.

The assessment of the existence of temporal trends in the frequencies of the air flow types over the whole study period has taken into account that seasonality and serial correlation are present, to a greater or lesser extent, in the time series. The analysis revealed significant trends in only a few cases, which show small trend magnitudes. Even if there exist some differences in the results of the three nonparametric methods considered (Table 2), they consistently detect a significant upward trend for Ns reaching Mace Head at 500 m, while negative trends are found for NWs reaching Málaga at 500 m and WSWs for Mace Head at 3000 m (see Figure 4). It should be noted that for the latter cases, the T-S slope of the original monthly time series is equal to 0, while it is negative for both the deseasonalized monthly series and the yearly ones. Weakly significant trends are found by some of the methods for N and WSW flows reaching Mace Head at 1500 m, thus showing some resemblance to the corresponding Ns at 500 m and WSWs at 3000 m.

The NAOi time series over the 20 year study period shows no significant trend according to the tests, despite both the

Table 2. Air Flow Types That Exhibit a Monotonic Trend Over the Whole Study Period, After Three Tests: Seasonal Kendall Test and Predeseasonalized Yue-Pilon (Y-P) Procedure for the Monthly Data and Mann-Kendall (M-K) Test for the Annual Means Time Series[a]

		Monthly Frequencies		Annual Frequencies
	Flow Type	Seasonal *K*	Deseasonalized + Y-P	M-K
		Mace Head		
3000 m	NW		0.0736(+)/1.33	
	WSW	**0.0433(−)/0.00**	**0.0472(−)/−1.39**	**0.0476(−)/−1.36**
1500 m	N	0.0781(+)/0.00	0.0768(+)/1.23	
	WSW			0.0548(−)/−0.56
500 m	N	**0.0186(+)/1.25**	**0.0157(+)/1.61**	0.0911(+)/1.73
		Málaga		
500 m	NW	0.0624(−)/0.00	**0.0458(−)/−0.66**	0.0782(−)/−0.96
	Wslow			0.0636(+)/1.11

[a]For each case, *p* value (sign of the trend)/Theil-Sen trend are given. In bold when significant at the 0.05 level; the rest of the flows present weak trends, i.e., significance at the 0.1 level.

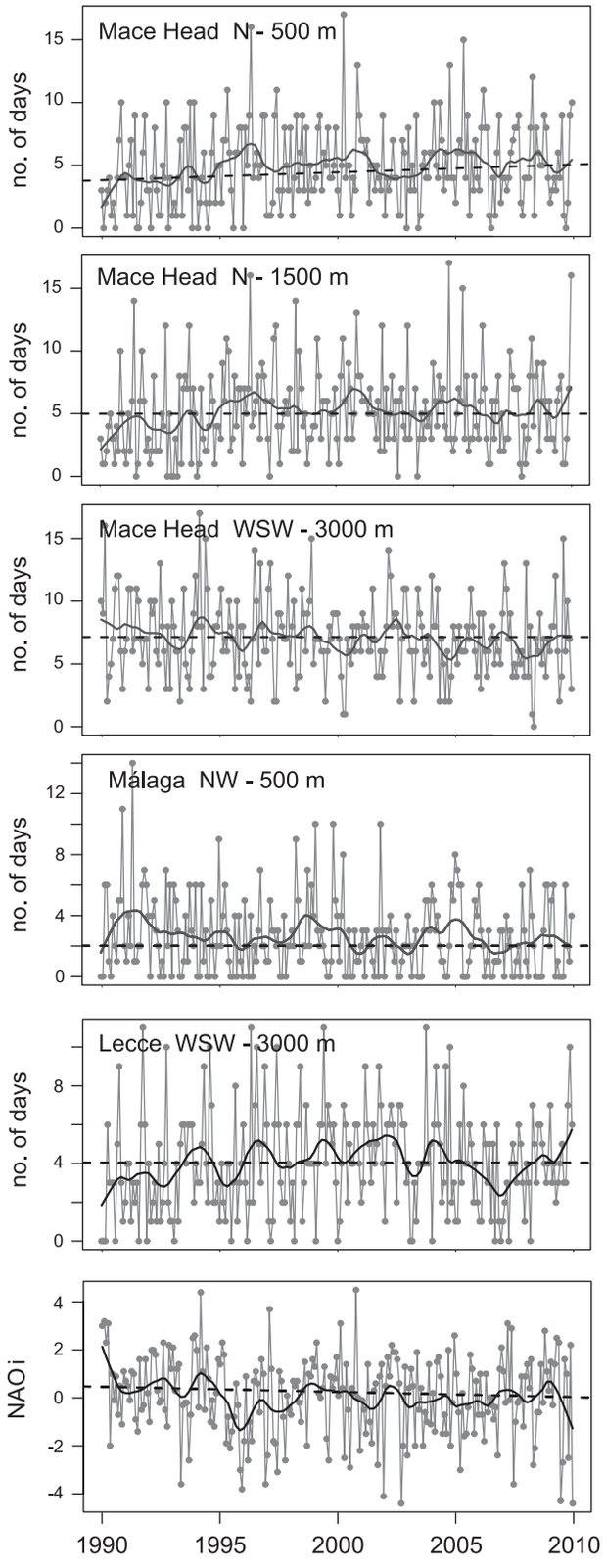

monthly time series (deseasonalized or not), and the yearly series presented a negative T-S slope.

The existence of trends in the studied 20 year period is relevant when comparing to other variables in the same period, but whether this period is representative or not of a longer-term trend can only be ascertained if longer data sets of trajectories were computed. The sensitivity of the trend estimates to choices in the start and end points of a time series increases, in general, with decreasing study period. When the seasonal Kendall test was applied to a rolling window of 10 years, the number of flow types showing significant trends increased. The periods that more frequently exhibited significant trends at Mace Head are 1990 (1991) to 1999 (2000) and 1996 (1997) to 2005 (2006). Moreover, northerlies reaching Mace Head at 500 and 1500 m show significant trends only for the periods starting in 1990, 1991, and 1992. However, other situations can be found: the negative trend shown by WSW flows reaching Mace Head at 3000 m over the 20 year period is not significant when examined over 10 year windows; and other flows present a positive trend that changes afterward to a negative one, as occurs to WSWs reaching Lecce at 3000 m.

A visual inspection of the time series and their trend components obtained from the seasonal-trend decomposition analysis (Figure 4) suggests that the overall trends shown by the frequencies of N flows at Mace Head and NWs at Málaga may be composed by a first stronger upward/downward trend until 1996 that leveled off thereafter. That would also be apparent in some air flow types for which the 1990–2009 trends were not significant, like Wfast flows arriving at 1500 and 3000 m at Mace Head (not shown). A two-piecewise trend analysis constrained to look for a significant trend in a first period and for no trend in a second one, both periods with varying start and end times, identified in most cases the periods 1990–1996 (22 air flow types showed significant trend) and 2001–2009 (only four flow types showed a significant trend), respectively; in between, there is an intermediate behavior. In particular, N flows at Mace Head exhibit an increase of 3.1 and 2.4 days over the 7 year period at 1500 and 500 m, respectively, as given by the T-S slope, NWs at Málaga show no significant trend in that period, and Wfast flows reaching Mace Head at 3000 and 1500 m present a slope of −3.15 and −3.84 days in that period, respectively.

Figure 4. (opposite) (first four plots) Evolution of the monthly frequency of occurrence of the air flow types that show significant trends over the whole study period, (fifth plot) a case presenting nonmonotonic trend and (bottom plot) evolution of the North Atlantic Oscillation index (NAOi). Dashed lines are the linear regressions with Theil-Sen slope estimate, and black solid lines are the local trends from the seasonal-trend decomposition analysis.

The NAOi time series shows a significant downward trend (T-S slope of −1.92 days in the 1990–1996 period) that is followed by stabilization from 2001 onward. It is unclear to us what the reason is for the different behavior up to 1996.

3.2. Association Between Variability in Air Flow Types and the NAO

Figure 5 shows the composite fields of the monthly 1000 and 700 hPa geopotential heights averaged over the positive and the negative phases of the NAO in the 20 year period; the left panels include all 12 months of the year, while the ones at the right are restricted to the extended-winter period (DJFM), which is frequently utilized in the literature of the NAO. No composites of geopotential height anomalies are displayed since the work is aimed to a direct comparison with advection pathways.

At 1000 hPa, a typical dipole spatial pattern is seen with the two NAO centers of action showing different intensities, locations, and spatial extent depending on the NAO phase. The meridional gradient of geopotential height observed at midlatitudes is the major feature found at 700 hPa. An upper-level ridge is located in the Atlantic façade of the European continent. Other synoptic systems are apparent in Figure 5, like the thermal low that frequently forms over northern Africa as well as the North African high, present at upper levels, which are reflected in the charts of the negative phase of the NAO for all 12 months.

The strengthening of the pressure centers during the positive NAO phase, results in an increased pressure gradient over the North Atlantic. Also, the two centers of action are located more north-eastward in the positive phase. It can be observed as well that variations in geopotential height are much larger in the Iceland low than in the Azores high when comparing the positive and negative phases of the NAO. It can also be seen that all these dissimilarities are enhanced in winter time.

Another overall feature is that the tilt of the upper-level ridge found at the eastern Atlantic is determined by the displacement and change in intensity of the Atlantic subtropical high but also by the presence of the African high.

The spatial differences between the two phases should be, at least qualitatively, of larger importance in the areas where the centers of action expand and contract; that would explain why most of the studies related to the NAO have been performed for Scandinavia and Iberia as indicated by *Beranová and Huth* [2007].

At the regional scale, there are strong differences between northern and southern locations. According to the composite charts in Figure 5, the westerly circulation in southwestern Europe is reduced by the influence of the subtropical high in the positive phase of the NAO, and easterlies/northeasterlies and situations of weak baric gradient are frequent at the lower levels. In contrast, at latitudes higher than 50°N, strong pressure gradients lead to westerlies that are stronger than average.

These are well-known features of the NAO. In order to relate the advection patterns found by the cluster analysis to the NAO, we examined the spatial footprint of the whole set of trajectory pathways according to either phase of the NAO, which can be compared to the composite synoptic situations. After this, the association between the variation of different advection patterns and the NAOi will be addressed.

Figure 6 displays the fraction of time that the air parcels remain in a 1° latitude-longitude grid cell for the extended-winter months (DJFM); positive and negative phases of the NAO are considered separately, and only months with positive NAOi in the fourth quartile and months with negative NAOi in the first quartile are considered.

It is readily observed that during the positive phase of the NAO, the pathways that correspond to polar maritime air masses reaching Mace Head and Cabauw are the most frequent ones, while arctic air masses as well as easterlies are more frequent in the negative phase. In the Mediterranean, the arrival of polar maritime air masses occurs more frequently in the positive phase of the NAO, while southwesterlies and purely zonal flows of lower speed are much less common than in the negative phase.

The correlation analysis between the NAOi and the frequencies of the flow types on a seasonal basis provides a quantitative assessment of their degree of association while reducing the effect of the month-to-month correlations. Table 3 shows the linear correlation coefficients for the cases having significant association during the DJFM months, with Pearson correlation coefficients in the range 0.93 to −0.79. The association is much stronger for the air flow types reaching Mace Head and Cabauw than for those reaching the Mediterranean and Lisbon: correlation coefficients and significance are the largest for Mace Head, whereas no significant association to the NAOi is found at Lisbon. Moreover, statistically significant correlations were found in 71% of the air flow types in Cabauw, 78% in Mace Head, 35% in Lecce, 22% in Málaga, 21% in Elche, and 0% in Lisbon. The location of Lisbon, under the direct influence of the subtropical high, may explain that reduced relationship.

There is a strong positive correlation at Mace Head and Cabauw between the NAOi and Wfast and WSW flows. This can be understood from the stronger pressure gradients found in the region during the positive phase of the NAO (composite maps of Figure 5), and it is directly related to the residence times of these maritime air masses (panels in the first row of Figure 6) during the positive phase. Correspondingly,

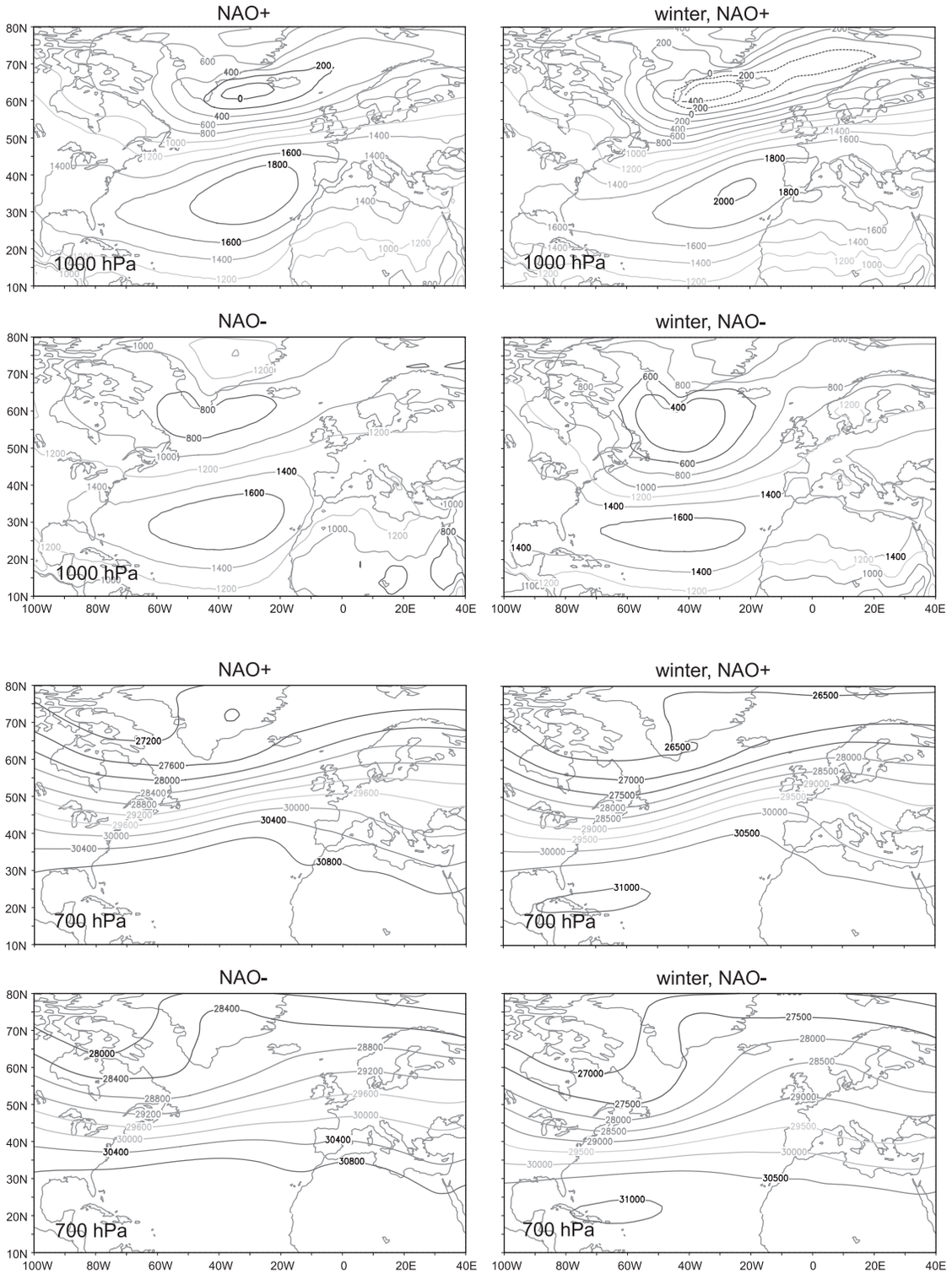

Figure 5. Charts of geopotential height at 1000 and 700 hPa averaged over the months with positive and negative NAO, computed from European Centre for Medium-Range Weather Forecasts reanalysis-Interim data (http://data-portal.ecmwf.int/data/d/interim_moda/). (left) Averages over all 12 months. (right) Averages over winter months. Contour increment is 200 (400) hPa for the 1000 (700) hPa charts.

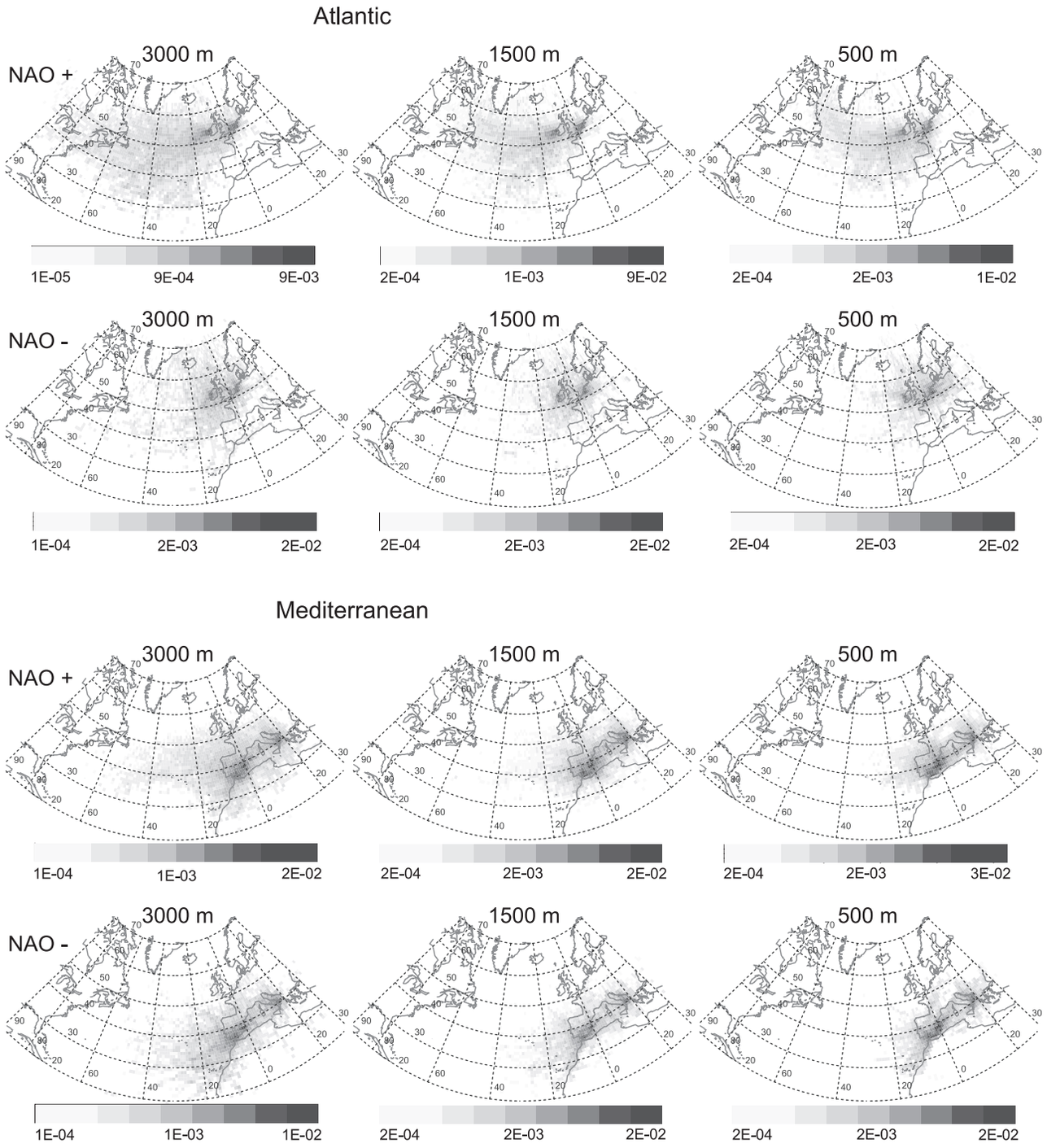

Figure 6. Overall residence time of air parcels reaching the northern study sites (two first rows) and the Mediterranean ones (two lasts rows) in the positive and the negative phases of the NAO in wintertime. The fraction of time that the air parcels reside at a grid point with respect to the total time spent by all air parcels is depicted.

Table 3. Pearson Correlation Coefficient for the Cases With Significant Association Between North Atlantic Oscillation Index and the Frequencies of the Air Flow Types at Each Location (DJFM Means)[a]

				Mace Head			
3000 m	**WSW**	**NW**	**Wfast**	SW	**E**		
	0.64	−0.54	**0.82**	–	**−0.71**		
1500 m	SW	**WSW**	**E**	**Wfast**	**N**	W	
	–	**0.74**	**−0.79**	**0.93**	**−0.63**	–	
500 m	SW	**Wfast**	**N**	**WSW**	W	**E**	
	–	**0.92**	−0.58	**0.66**	–	**−0.74**	
				Cabauw			
3000 m	**Wfast**	**WSW**	W	**E**	**SW**	**NW**	
	0.83	**0.75**	–	−0.58	−0.53	−0.59	
1500 m	**N**	**WSW**	W	**SW**	**E**	**Wfast**	
	−0.51	0.60	–	**−0.56**	**−0.68**	**0.80**	
500 m	SW	**Wfast**	N	**WSW**	W	**E**	
	−0.49	**0.88**	–	0.59	–	**−0.76**	
				Lecce			
3000 m	W	SW	**NWfast**	NW	NE	Wfast	**WSW**
	–	−0.41	**0.77**	–	–	–	−0.57
1500 m	NE	Wfast	S	**NWfast**	NW	WSW	W
	–	–	–	**0.70**	–	−0.38	–
500 m	NWslow	NE	NW	**NWfast**	W	S	
	–	–	–	**0.58**	−0.40	–	
				Lisbon			
3000 m	NWfast	NE	SW	W	NW	Wfast	
	–	–	–	–	–	–	
1500 m	NWfast	E	NW	SW	W		
	–	–	–	–	–		
500 m	E	NWfast	NW	Wslow	W		
	–	–	–	–	–		
				Elche			
3000 m	NWfast	W	E	NW	SW		
	–	−0.38	–	–	–		
1500 m	W	NW	NWfast	E	Wslow		
	−0.40	–	–	–	–		
500 m	NWfast	NW	W	E			
	–	–	−0.40	–			
				Málaga			
3000 m	NWfast	SW	W	NW	S	N	Wfast
	–	−0.31	–	–	0.38	–	–
1500 m	NWfast	E	NW	W	SW		
	–	0.38	–	–	–		
500 m	W	NW	Wslow	E	NWslow	NWfast	
	−0.41	–	–	–	–	–	

[a]Significance at the 0.01 level in both linear and Kendall tests (air flow type and correlation value in bold), at the 0.05 level in both tests (air flow type only in bold), and cases with significance at the 0.1 level at least in one of the tests.

E and NW/N flows are strongly anticorrelated with NAOi, and residence time plots in the second row of Figure 6 show their association to the negative phase of the NAO. SW flows reaching Cabauw are also anticorrelated with the NAOi.

In the central Mediterranean, fast polar maritime air masses (NWfast flows) are positively correlated with the NAOi, just like in the northern Atlantic locations. This is, however, not observed in the western Mediterranean during the extended-winter period. In turn, W flows reaching the three Mediterranean sites at low levels are anticorrelated with the NAOi, as are WSWs in Lecce and SWs in Málaga above the atmospheric boundary layer. That means that the displacement of the

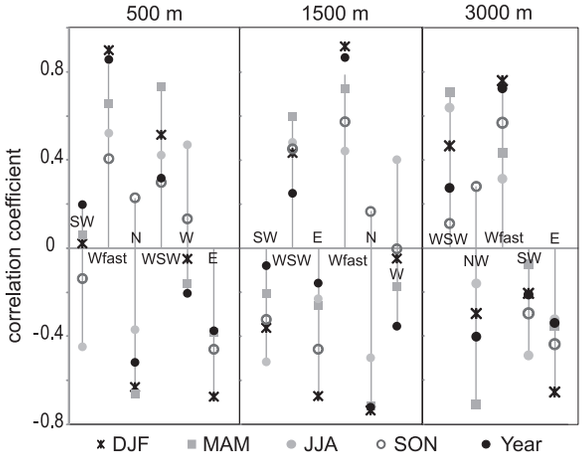

Figure 7. Pearson correlation coefficients between the frequency of occurrence of the different air flow types and the NAOi, by season and for the full year, for Mace Head. The vertical lines are just a guide to the eye.

subtropical high at lower latitudes during the negative phase of the NAO facilitates the entrance of westerlies/southwesterlies to the Mediterranean, which can be observed in the residence time plots of Figure 6. The frequency of easterly flows in the Mediterranean is not associated to the NAOi, with the exception of Málaga where correlation is positive. In this location, the shift and strengthening of the Azores high induces anticyclonic circulation with easterly component (Figure 5). Finally, some association of southern flows during the positive phase of the NAO is observed in Málaga.

Given that Mace Head exhibits the highest correlation coefficients, the association between the air flow types at this location and the NAOi was further analyzed by season (Figure 7). No significant differences in correlations are found when studying the extended-winter or the winter periods. Furthermore, the association between each air flow type and the NAO is similar at the different seasons, with only two exceptions: westerlies, which are positively correlated in summertime, and northerlies, which present a weak positive correlation in autumn. As shown in Figure 7, winter and spring seasons present the most extreme correlation coefficients, positive for Wfast and WSW flows and negative for N and E (this last case only in wintertime) advections. More moderate correlations are found in summertime, which exhibits the strongest association between the NAOi and SWs and NAOi and Ws (negative and positive correlations, respectively).

4. DISCUSSION AND CONCLUSIONS

This paper presents a classification of the main pathways of advection to six locations in western Europe over an extended period of time, as well as its analysis in terms of temporal trends and association to a regional circulation index. While this kind of analysis is usually performed in a context where synoptic circulation/weather type classifications are utilized, the exploratory study presented here demonstrates the feasibility of the approach.

Air flow types have been identified by cluster analysis of back trajectories. The trajectory analysis may reveal the main features of the pathways followed by the flows reaching a specific location, as well as highlight differences between sites. It should also be noted that the time evolution of the wind fields is embodied in the trajectory pathway.

Temporal trends and association to NAOi were examined on a monthly basis from the frequencies of occurrence of each transport pattern. Aside from a purely climatological application, our final interest is the interpretation of atmospheric composition observations in relation to advection patterns, which needs a clear understanding of the temporal variability of the flows reaching the study site.

Two Atlantic locations at higher latitudes, as well as Lisbon and three Mediterranean sites were considered; the use of the same methodology and meteorological database assures results between the six locations are comparable. A different number of advection pathways have been found at each location. Overall, results reflect strong seasonal pattern with prevalence of westerlies and the association of NAOi to known synoptic situations. However, such association varies strongly between locations due to latitudinal differences and the closeness to the subtropical high and also to those implied by the relief in the Mediterranean basin. Most of the air flow types at Cabauw and Mace Head are significantly correlated to the NAOi, while at Lisbon (especially), Elche, and Málaga, they appear to be almost decoupled from the NAO, with only W flows being associated to the negative phase of the NAO. Málaga is under the influence of westerlies and easterlies passing over the Strait of Gibraltar, which are positively correlated to the positive and negative, respectively, phases of the NAO. Westerly influences at Lecce are associated to NWfast flows in the positive phase of the NAO and to WSW advections that pass over the western Mediterranean in the negative phase.

Significant temporal trends are found for a few air flow types at Mace Head and Málaga. Over the 20 year period, WSW flows arriving at the lower free troposphere at Mace Head present a steady significant decreasing trend. The rest of the significant trends are associated to northerly flows and level off from 2000 onwards, as it is observed in the NAOi time series.

There is a vast number of extensions to this work. According to the final motivation of this work, the analysis of long-term series of meteorological parameters or the

concentrations of atmospheric constituents registered at a given location (like ozone concentrations at Mace Head or precipitation data in southern Spain) can be done in relation to the variability of air flow frequencies and the NAOi at various time scales.

The cluster analysis can include the information of the altitude along the trajectory pathway, which could give more insight on the relation between air flow types and other meteorological and air quality data. Besides, cluster analysis may be restricted to winter trajectories only, given the more pronounced influence of the NAO in that period; results might highlight some subtle differences in advection patterns in that season. In addition, LPD models could be used instead of the single trajectory approach, though the computational cost involved in studying periods of a few decades should be considered.

There is no characteristic time scale of variability for the NAO and daily, monthly, seasonal, winter, and annual NAOi are used in the literature. Variability at different time scales can be readily studied from the daily classification of transport pathways. Of course, the analysis is not restricted to the NAOi; other regional or global circulation indices may show association with the frequencies of the advection patterns, which would be worth studying.

Acknowledgments. The authors would like to thank the anonymous reviewers for their valuable comments and suggestions. This study was partially supported by the Spanish Ministry of Education and Science, project CGL2008-05160 (EroHondo).

REFERENCES

Almeida, S. M., C. A. Pio, M. C. Freitas, M. A. Reis, and M. A. Trancoso (2005), Source apportionment of fine and coarse particulate matter in a sub-urban area at the Western European Coast, *Atmos. Environ.*, *39*, 3127–3138.

Arnold, D., A. Vargas, A. T. Vermeulen, B. Verheggen, and P. Seibert (2010), Analysis of radon origin by backward atmospheric transport modeling, *Atmos. Environ.*, *44*, 494–502.

Ashbaugh, L. L., W. C. Malm, and W. Z. Sadeh (1985), A residence time probability analysis of sulfur concentrations at Grand Canyon National Park, *Atmos. Environ.*, *19*, 1263–1270.

Beranová, R., and R. Huth (2007). Time variations of the relationships between the North Atlantic Oscillation and European winter temperature and precipitation, *Stud. Geophys. Geod.*, *51*, 575–590, doi:10.1007/s11200-007-0034-3.

Brankov, E., S. T. Rao, and P. S. Porter (1998), A trajectory-clustering-correlation methodology for examining the long-range transport of air pollutants, *Atmos. Environ.*, *32*, 1525–1534.

Cabello, M., J. A. G. Orza, and V. Galiano (2008), Air mass origin and its influence over the aerosol size distribution: A study in SE Spain, *Adv. Sci. Res.*, *2*, 47–52.

Cape, J. N., J. Methven, and L. E. Hudson (2000), The use of trajectory cluster analysis to interpret trace gas measurements at Mace Head, Ireland, *Atmos. Environ.*, *34*, 3651–3663.

Cleveland, R. B., W. S. Cleveland, J. E. McRae, and I. Terpenning (1990), STL: A seasonal-trend decomposition procedure based on Loess, *J. Off. Stat.*, *6*, 3–73.

Dee, D. P., et al. (2011), The ERA-Interim reanalysis: Configuration and performance of the data assimilation system, *Q. J. R. Meteorol. Soc.*, *137*, 553–597, doi:10.1002/qj.828.

Delcloo, A. W., and H. De Backer (2008), Five day 3D back trajectory clusters and trends analysis of the Uccle ozone sounding time series in the lower troposphere (1969–2001), *Atmos. Environ.*, *42*, 4419–4432.

Dorling, S. R., T. D. Davies, and C. E. Pierce (1992). Cluster analysis: A technique for estimating the synoptic meteorological controls on air and precipitation chemistry – Method and applications, *Atmos. Environ., Part A*, *26*, 2575–2581.

Draxler, R. R., and G. D. Hess (1998), An overview of the HYSPLIT_4 modeling system of trajectories, dispersion, and deposition, *Aust. Meteorol. Mag.*, *47*, 295–308.

Dueñas, C., J. A. G. Orza, M. Cabello, M. C. Fernández, S. Cañete, M. Pérez, and E. Gordo (2011), Air mass origin and its influence on radionuclide activities (7Be and 210Pb) in aerosol particles at a coastal site in the western Mediterranean, *Atmos. Res.*, *101*, 205–214.

Henne, S., D. Brunner, D. Folini, S. Solberg, J. Klausen, and B. Buchmann (2010), Assessment of parameters describing representativeness of air quality in-situ measurement sites, *Atmos. Chem. Phys.*, *10*, 3561–3581.

Hirsch, R. M., J. R. Slack, and R. A. Smith (1982), Techniques of trend analysis for monthly water quality data, *Water Resour. Res.*, *18*(1), 107–121.

Hondula, D. M., L. Sitka, R. E. Davis, D. B. Knight, S. D. Gawtry, M. L. Deaton, T. R. Lee, C. P. Normile, and P. J. Stenger (2010), A back-trajectory and air mass climatology for the Northern Shenandoah Valley, USA, *Int. J. Climatol.*, *30*, 569–581.

Hurrell, J. W. (1995), Decadal trends in the North Atlantic Oscillation: Regional temperatures and precipitation, *Science*, *269*, 676–679.

Hurrell, J. W., and H. van Loon (1997), Decadal variations in climate associated with the North Atlantic Oscillation, *Clim. Change*, *36*, 301–326.

Jones, P. D., T. J. Osborn, and K. R. Briffa (2003), Pressure-based measures of the North Atlantic Oscillation (NAO): A comparison and an assessment of changes in the strength of the NAO and in its influence on surface climate parameters, in *The North Atlantic Oscillation: Climatic Significance and Environmental Impact*, *Geophys. Monogr. Ser.*, vol. 134, edited by J. W. Hurrell et al., pp. 51–62, AGU, Washington, D. C., doi:10.1029/134GM03.

Jorba, O., C. Pérez, F. Rocadenbosch, and J. M. Baldasano (2004), Cluster analysis of 4-day back trajectories arriving in the Barcelona Area, Spain, from 1997 to 2002, *J. Appl. Meteorol.*, *43*, 887–901.

Kahl, J. D. W., D. A. Martinez, H. Kuhns, C. I. Davidson, J.-L. Jaffrezo, and J. M. Harris (1997), Air mass trajectories to Summit, Greenland: A 44-year climatology and some episodic events, *J. Geophys. Res.*, *102*, 26,861–26,875.

Lorenzo, M. N., J. J. Taboada, and L. Gimeno (2008), Links between circulation weather types and teleconnection patterns and their influence on precipitation patterns in Galicia (NW Spain), *Int. J. Climatol.*, *28*, 1493–1505.

Markou, M. T., and P. Kassomenos (2010). Cluster analysis of five years of back trajectories arriving in Athens, Greece, *Atmos. Res.*, *98*, 438–457.

Moody, J. L., and J. N. Galloway (1988), Quantifying the relationship between atmospheric transport and the chemical composition of precipitation on Bermuda, *Tellus, Ser. B*, *40*, 463–479.

Pozo-Vázquez, D., M. J. Esteban-Parra, F. S. Rodrigo, and Y. Castro-Díez (2000), An analysis of the variability of the North Atlantic Oscillation in the time and the frequency domains, *Int. J. Climatol.*, *20*, 1675–1692.

R Development Core Team (2010), R: A language and environment for statistical computing, http://www.R-project.org, R Found. for Stat. Comput., Vienna.

Santese, M., F. de Tomasi, and M. R. Perrone (2008), Advection patterns and aerosol optical and microphysical properties by AERONET over south-east Italy in the central Mediterranean, *Atmos. Chem. Phys.*, *8*, 1881–1896.

Sheridan, S. C. (2003), North American weather-type frequency and teleconnection indices, *Int. J. Climatol.*, *23*, 27–45.

Stohl, A. (1996), Trajectory statistics—A new method to establish source-receptor relationships of air pollutants and its application to the transport of particulate sulfate in Europe, *Atmos. Environ.*, *30*, 579–587.

Stohl, A. (1998), Computation, accuracy and applications of trajectories—A review and bibliography, *Atmos. Environ.*, *32*, 947–966.

Stohl, A., and P. Seibert (1998), Accuracy of trajectories as determined from the conservation of meteorological tracers, *Q. J. R. Meteorol. Soc.*, *124*, 1465–1484.

Stohl, A., and P. James (2004). Lagrangian analysis of the atmospheric branch of the global water cycle. Part I: Method description, validation, and demonstration for the August 2002 flooding in Central Europe, *J. Hydrometeorol.*, *5*, 656–678.

Tripathi, O. P., S. G. Jennings, C. D. O'Dowd, L. Coleman, S. Leinert, B. O'Leary, E. Moran, S. J. O'Doherty, and T. G. Spain (2010), Statistical analysis of eight surface ozone measurement series for various sites in Ireland, *J. Geophys. Res.*, *115*, D19302, doi:10.1029/2010JD014040.

Vermeulen, A. T., A. Hensen, M. E. Popa, W. C. M. van den Bulk, and P. A. C. Jongejan (2011), Greenhouse gas observations from Cabauw Tall Tower (1992–2010), *Atmos. Meas. Tech.*, *4*, 617–644.

Yue, S., P. Pilon, B. Phinney, and G. Cavadias (2002), The influence of autocorrelation on the ability to detect trend in hydrological series, *Hydrol. Processes*, *16*, 1807–1829.

M. Cabello, V. Galiano, and J. A. G. Orza, SCOLAb, Física Aplicada, Universidad Miguel Hernández, Elche E03202, Spain. (ja.garcia@umh.es)

A. F. Stein, Air Resources Laboratory, NOAA, Silver Spring, MD 20910, USA.

A. T. Vermeulen, Environmental Assessment, ECN-Energy Research Centre of the Netherlands, Petten 1755 LE, Netherlands.

ECN
Westerduinweg 3
1755 LE Petten

Postbus 1
1755 LG Petten

T 088 515 4949
F 088 515 8338
info@ecn.nl
www.ecn.nl